Pakistan Veterinary Journal

ISSN: 0253-8318 (PRINT), 2074-7764 (ONLINE)
DOI: 10.29261/pakvetj/2026.239

RESEARCH ARTICLE

# STAT3 Mediates Resistance to Pseudorabies Virus Infection in a Phosphorylation-Dependent Manner

Shasha Liu[1,2,3#], Feng Qiu[1,2#], Haiyang Zhang[1,2#], Feiyang Xu[1,2], Beining Weng[1,2], Zhengdan Ai[1,2], Ruijing Su[1,2,3*] and Hongxiu Diao[1,2,3*]

[1]Key Laboratory of Animal Pathogen Infection and Immunology of Fujian Province, College of Animal Sciences, Fujian Agriculture and Forestry University, Fuzhou 350002, China; [2]Key Laboratory of Fujian-Taiwan Animal Pathogen Biology, College of Animal Sciences, Fujian Agriculture and Forestry University, Fuzhou 350002, China; [3]Joint Laboratory of Animal Pathogen Prevention and Control of Fujian-Nepal, College of Animal Sciences, Fujian Agriculture and Forestry University, Fuzhou 350002, China
*Corresponding author: suruijing@fafu.edu.cn (RS); diaohongxiu@yeah.net (HD)

ARTICLE HISTORY (26-884)

Received: July 23, 2026
Revised: September 02, 2026
Accepted: September 04, 2026
Published online: October 17, 2026

**Key words:**
Innate immunity
Interleukin-6
Phosphorylation
Pseudorabies virus
STAT3

**ABSTRACT**

Pseudorabies virus (PRV) imposes heavy economic burdens on the worldwide pig industry. STAT3 is a well-established regulator of antiviral immunity; however, its functional roles and underlying mechanisms during PRV infection remain poorly defined. Here, we observed that PRV infection robustly induces STAT3 phosphorylation. We further characterized the functional contribution of STAT3 to PRV replication. Our results demonstrated that knockdown of STAT3 markedly facilitates PRV replication, whereas overexpression of wild-type STAT3 ($STAT3^{WT}$) significantly suppresses viral replication. Consistently, the constitutively active STAT3 ($STAT3^{D661V}$) inhibits PRV replication, while the dominant-negative mutant STAT3 ($STAT3^{Y705F}$) strongly enhances viral replication. *In vivo* assays further confirmed that PRV replication is greatly elevated in $STAT3^{Y705F/+}$ mice. Mechanistically, STAT3 modulates PRV replication by positively regulating critical innate antiviral genes, including IFITM1, IFIT2, and ISG15. STAT3 knockdown reduces the expression of these genes; conversely, overexpression of $STAT3^{WT}$ or $STAT3^{D661V}$ elevates them, and disruption of STAT3 Y705 diminishes their expression. Moreover, STAT3 modulates the production of the pro-inflammatory cytokine interleukin-6 (IL-6) upon PRV infection. Collectively, these findings reveal that STAT3-mediated innate immune responses are essential for host defense against PRV infection, highlighting its capacity to restrict PRV replication via regulating antiviral genes expression and IL-6 production.

**To Cite This Article:** Liu S, Qiu F, Zhang H, Xu F, Weng B, Ai Z, Su R and Diao H, 2026. STAT3 mediates resistance to pseudorabies virus infection in a phosphorylation-dependent manner. Pak Vet J, 46(10): 2487-2498. http://dx.doi.org/10.29261/pakvetj/2026.239

## INTRODUCTION

Pseudorabies virus (PRV) is an enveloped, neurotropic double-stranded DNA virus belonging to the family *Herpesviridae*, subfamily *Alphaherpesvirinae*, and genus *Varicellovirus*. Its genome spans approximately 143 kb, encoding over 70 viral proteins (Liu *et al.*, 2022a; Ye *et al.*, 2023). The clinical outcomes of PRV infection vary substantially with host age. Newborn piglets primarily develop fatal central nervous system disorders, predominantly encephalitis, with mortality approaching 100%, whereas adult pigs mainly exhibit respiratory distress and reproductive dysfunction (Laval and Enquist *et al.*, 2020; Chen *et al*., 2023). Beyond swine, various other mammals are susceptible to PRV infection, including cattle, sheep, cats, dogs, and wildlife (Musante *et al.,* 2014; Papageorgiou *et al.*, 2024). Increasing evidence suggests that humans are also potentially susceptible to PRV infection. Although several suspected human cases have been reported (Liu *et al.*, 2022c; Wang *et al.*, 2024), only a few cases have been confirmed through high-throughput viral genome sequencing (Yan *et al.,* 2023). PRV glycoprotein gD mediates viral entry into human cells by interacting with the nectin-1 receptor. This gD protein is highly conserved among porcine PRV variants and exhibits comparable binding affinity for

human and porcine nectin-1 (Zhang *et al.*, 2011; Li *et al.*, 2017). In addition, the PRV tegument protein UL21 has been identified as a potent suppressor of host innate immune responses. Mechanistically, UL21 triggers cGAS degradation through TOLLIP-dependent selective autophagy (Ma *et al.*, 2023).

The innate immune system serves as the first line of defense against viral invasion. Upon recognition of pathogen-associated molecular patterns (PAMPs) by host pattern recognition receptors (PRRs), interferons (IFNs) and pro-inflammatory cytokines are produced to jointly constrain viral infection and replication (Holicek *et al.*, 2024; Neurath *et al.,* 2024). Specifically, ligation of type I IFNs to their receptors (IFNAR1 and IFNAR2) activates the JAK-STAT signaling cascade, leading to the expression of abundant IFN-stimulated genes (ISGs) (Yin *et al.*, 2021; Wang *et al.*, 2024). Among these ISGs, ISG15 is upregulated during PRV infection and suppresses viral replication by enhancing IFN-β production (Zhang *et al.*, 2021). Consistently, ISG15-knockout mice exhibit enhanced susceptibility to PRV infection (Li *et al*., 2022). Mechanistically, ISG15 promotes the assembly of STAT1/STAT2/IRF9 complex (ISGF3) and enhances ISGF3-dependent transcriptional activation, thereby strengthening type I IFN-mediated anti-PRV responses (Liu *et al.*, 2022b). OASL is another critical ISG with anti-PRV function. Chen *et al.* found that OASL constrains PRV replication by amplifying RIG-I signaling and driving RIG-I-dependent IFN production. To circumvent this host defense, PRV utilizes its UL24 protein to repress OASL transcription, thereby dampening RIG-I signaling and abrogating the OASL-mediated antiviral effect (Chen *et al.*, 2021). Furthermore, IFITM proteins are key restrictive factors for PRV infection. IFITM1 confers strong anti-PRV activity, as IFITM1 knockdown increases PRV titers, whereas IFITM1 overexpression impedes PRV cellular entry (Wang *et al.*, 2020). Differently, IFITM2 restricts PRV infection by inhibiting viral binding and entry in a cholesterol-dependent manner (Xie *et al.,* 2020).

STAT3 participates in a wide range of critical biological processes, including cell survival, differentiation, proliferation, and cell-cycle regulation (Zou *et al.*, 2020; Hu *et al.*, 2024). For instance, STAT3 enhances the effector functions of $CD8^+$ T cells against herpes simplex virus type 1 (HSV-1) infection (Roca Suarez *et al.*, 2018; Faust *et al.*, 2025). Following viral invasion, STAT3 is selectively activated by type I IFN in multiple cell types and negatively modulates the type I IFN response (Wang *et al.*, 2011). Studies have shown that induced phosphorylation of STAT3 at the Y705 site regulates antiviral immune responses during the early stage of influenza virus infection (Liu *et al.,* 2023). Furthermore, STAT3 inhibits viral replication by inducing distinct subsets of ISGs (Mahony *et al.*, 2017). Silencing STAT3 not only promotes the replication of vaccinia virus and influenza virus but also impedes the induction of ISGs, such as PKR, OAS2, and ISG15 (Mahony *et al.*, 2017; Yoshida *et al.*, 2024). Moreover, STAT3 acts as a central target manipulated by viruses for immune evasion. For instance, hepatitis C virus (HCV) impairs type I IFN pathway by promoting STAT3 ubiquitination, which further substantiates the potential antiviral function of STAT3 (Oda *et al.*, 2025). Although STAT3 functions as a modulator of inflammation and tissue regeneration upon diverse pathogenic infections, its functional role during PRV infection remains poorly defined.

Notably, our study identified that PRV infection significantly induced STAT3 phosphorylation. Knockdown of STAT3 promoted PRV replication, whereas overexpression of STAT3 or constitutively active STAT3 inhibited it. Conversely, the dominant-negative mutant $STAT3^{Y705F}$ enhanced PRV replication both *in vitro* and *in vivo*. Mechanistically, activated-STAT3 upregulated antiviral genes (IFITM1, IFIT2, and ISG15) and IL-6 production. Our study demonstrates that phosphorylation-dependent STAT3 signaling restricts PRV replication by mediating host innate immune responses.

## MATERIALS AND METHODS

**Cell lines and cell culture:** Cell lines PK-15 (swine kidney), 3D4/21 (porcine alveolar macrophage), A549 (human alveolar adenocarcinoma), 293T (human embryonic kidney), L929 (mouse fibroblast), C57/B6-L (murine lung fibroblast), and NIH/3T3 (mouse embryonic fibroblast) were purchased from ATCC. All cells were cultured in Dulbecco's modified Eagle's medium (DMEM) supplemented with 10% fetal bovine serum (FBS) and 100U/mL penicillin-streptomycin (Beyotime Biotechnology, China), and maintained at 37°C with 5% $CO_2$ as previously described (Chi *et al.*, 2024).

**Viruses and viral infection:** PK-15 cells were used for propagation of PRV strain Min-A. 3D4/21, A549, 293T, L929, and NIH/3T3 cells were subjected to PRV infection. Cells were incubated with the virus for 1h and subsequently cultured in DMEM for the indicated time periods.

**Plaque-forming assay:** PK-15 cells were seeded one day prior to the experiment to achieve the appropriate density for virus inoculation. After PRV infected A549 cells for 12h, the supernatant (SNs) from the culture medium was collected for gradient dilution and then added to PK-15 cells for adsorption for 1h. Following adsorption, the wells were washed with PBS, and an equal volume of 2% methylcellulose (Promega, USA) mixed with culture medium was added to each well. The plate was incubated for 2-3 days at 37°C until distinct plaques formed. After removal of the overlay, the plaques were examined.

**Cell stimulation:** Recombinant human IL-6 was acquired from PeproTech (USA), and cells were treated as recommended by the manufacturer.

**RNA preparation, RT-PCR, and quantitative real-time PCR:** TRIzol reagent (Tiangen, China) was used for total RNA extraction following the manufacturer's protocol. The HiScript III 1st Strand cDNA Synthesis Kit (Vazyme, China) was employed to generate cDNA. Taq DNA polymerase (GenStar, China) was used for conventional PCR, and SYBR Green Master Mix (Vazyme, China) for qRT-PCR. Primer sequences are

shown in Table 1. GAPDH was selected as the reference gene, and relative RNA expression was determined by the 2-ΔΔCt method described earlier (Ma *et al.*, 2022).

**Antibodies and Western blotting:** Cell lysis was performed in radioimmunoprecipitation assay (RIPA) buffer containing protease inhibitors. After three washes with lysis buffer, immunoprecipitates were resolved by SDS-PAGE and transferred to nitrocellulose membranes for immunoblotting with designated antibodies as previously described (Wang *et al.*, 2016). The primary antibodies used: anti-phospho-STAT3(Y705) (CST, #9145, 1:2 000), anti-STAT3 (CST, #4904, 1:3 000), anti-Flag (Sigma, #F3165, 1:1 000), anti-β-actin (Santa Cruz, #sc-47778, 1:2 000).

**Animal experiments:** Wild-type (WT) BALB/c mice (5-6 weeks, 18-21g) were purchased from Shanghai SLAC Laboratory Animal Co., Ltd. (Shanghai, China). $STAT3^{Y705F/+}$ mice on the BALB/c background were used as previously described (Liu *et al.*, 2023). PRV ($5\times10^4$ plaque forming unit (PFU)) was delivered via intranasal inoculation. Mice were sacrificed at designated time points after infection for further assays.

**Statistical analysis:** Data shown are representative of three independent experiments yielding comparable results. Group differences were analyzed by the t-test using GraphPad Prism 9.5.0. Statistical significance was defined as $p < 0.05$.

**Table 1:** Primer sequences used for RT-PCR and qRT-PCR

| Primer name | Primer sequence（5'→3'） |
|---|---|
| PRV-gE (F) | TTTGGATCCATGCGGCCCTTTCTG |
| PRV-gE (R) | TTTGAATTCTTACGACACGGCGTCGCA |
| PRV-gD (F) | CTGATCTCCGACCCGCAG |
| PRV-gD (R) | GTACTGGCCCTCGTTGAACC |
| PRV-gI (F) | GTCCGTAGCCTCCGCAGT |
| PRV-gI (R) | CGCCACCCACAAAAT |
| IFITM2 (F) | CGGCCAGCCTCCCAACTAC |
| IFITM2 (R) | GCTGGGCCTGGACGACCAA |
| IFIT2 (F) | AGCGAAGGTGTGCTTTGAGA |
| IFIT2 (R) | GAGGGTCAATGGCGTTCTGA |
| ISG15 (F) | GACCTGACGGTGAAGATGCTG |
| ISG15 (R) | TGCTGCGGCCCTTGTTAT |
| IL-6 (F) | AATGAGGAGACTTGCCTGGTG |
| IL-6 (R) | TGAGGTGCCCATGCTACATT |

## RESULTS

**Phosphorylation of STAT3 at Y705 can be induced during PRV infection:** Our previous work demonstrated that PRV induces early STAT3 phosphorylation in PK-15 cells (Liu *et al.*, 2023). In agreement with this finding, we observed PRV-triggered Y705-phosphorylated STAT3 (pSTAT3) in porcine alveolar macrophage 3D4/21 cells (Fig. 1A). Recent studies have indicated that PRV can cross species barriers to infect humans (Mohiuddin *et al.*, 2023). To further clarify the role of STAT3 during PRV infection, we infected human 293T cells with PRV. As presented in Fig. 1B, marked elevation of pSTAT3 was detected as early as 2h post-infection (pi). Similarly, STAT3 phosphorylation was first observed at 4hpi in A549 cells (Fig. 1C and 1D).

To verify whether PRV-triggered STAT3 phosphorylation is a general phenomenon, we performed additional experiments in the mouse fibroblast NIH/3T3 cell line. PRV infection elicited a time-dependent increase in STAT3 phosphorylation in NIH/3T3 cells (Fig. 1E and 1F). Consistently, PRV also induced pSTAT3 in murine lung fibroblast C57/B6-L cells (Fig. 1G). To extend these *in vitro* findings to an *in vivo* setting, BALB/c mice were intranasally inoculated with PRV. pSTAT3 was detected in lung tissues at 8hpi, peak at 12-36hpi, and gradually declined during late-stage infection (Fig. 1H).

Collectively, these findings confirm that PRV infection is capable of inducing STAT3 phosphorylation in both cellular *in vitro* models and animal *in vivo* models.

**STAT3 could effectively inhibit the replication of PRV:** To investigate the function of STAT3 during PRV infection, we generated a STAT3-knockdown A549 cell line. As shown in Fig. 2A and 2B, this cell line exhibited efficient gene silencing. This knockdown cell line was therefore utilized for subsequent PRV-infection experiments. Our results revealed that mRNA levels of PRV-gE, which encodes a key structural protein responsible for PRV replication and virulence, were markedly elevated in STAT3-knockdown A549 cells compared with control cells (Fig. 2C). Further quantitative verification confirmed these results, showing that the mRNA levels of PRV-gE and PRV-gD in the silencing group were higher than in the control group (PRV-gE, Fold-changes=3.54; PRV-gD, Fold-changes=1.28; Fig. 2D and 2E). Consistently, the plaque assay demonstrated that STAT3 depletion markedly increased viral titers in A549 cells relative to control cells (Fold-changes=1.57, Fig. 2F). These results demonstrate that STAT3 can significantly inhibit the replication of PRV in A549 cells.

To further probe the role of STAT3, we generated a stable STAT3-overexpressing A549 cell line (Fig. 2G and 2H). The data revealed that STAT3 overexpression significantly decreased the mRNA levels of PRV-gE and PRV-gD in PRV-infected cells (Fig. 2I). Subsequent qRT-PCR analysis further validated that STAT3 overexpression markedly suppressed PRV-gE (Fold-changes=0.33) and PRV-gD (Fold-changes=0.44) mRNA expression (Fig. 2J and 2K). Additionally, viral titers were significantly lower in STAT3-overexpressing A549 cells than those in empty vector (EV)-control cells (Fold-changes=0.72, Fig. 2L). Collectively, these findings illustrate that STAT3 exerts robust inhibitory activity against PRV replication in A549 cells.

**Constitutively active STAT3 markedly suppresses PRV replication:** To further characterize STAT3-mediated anti-PRV activity, we transfected A549 cells with a constitutively active STAT3 mutant plasmid ($STAT3^{D661V}$) (Fig. 3A), as previously characterized (Gu *et al.*, 2025). In line with our above observations, mRNA levels of PRV-gE and PRV-gD were significantly reduced in $STAT3^{D661V}$-overexpressing A549 cells relative to control cells (Fig. 3B). qRT-PCR further validated these findings, revealing highly consistent changes (PRV-gE, Fold-changes=0.69; PRV-gD, Fold-changes=0.62; Fig. 3C and 3D). In addition, STAT3-constitutively active cells exhibited significantly lower viral titers compared with control cells (Fold-changes=0.59, Fig. 3E).

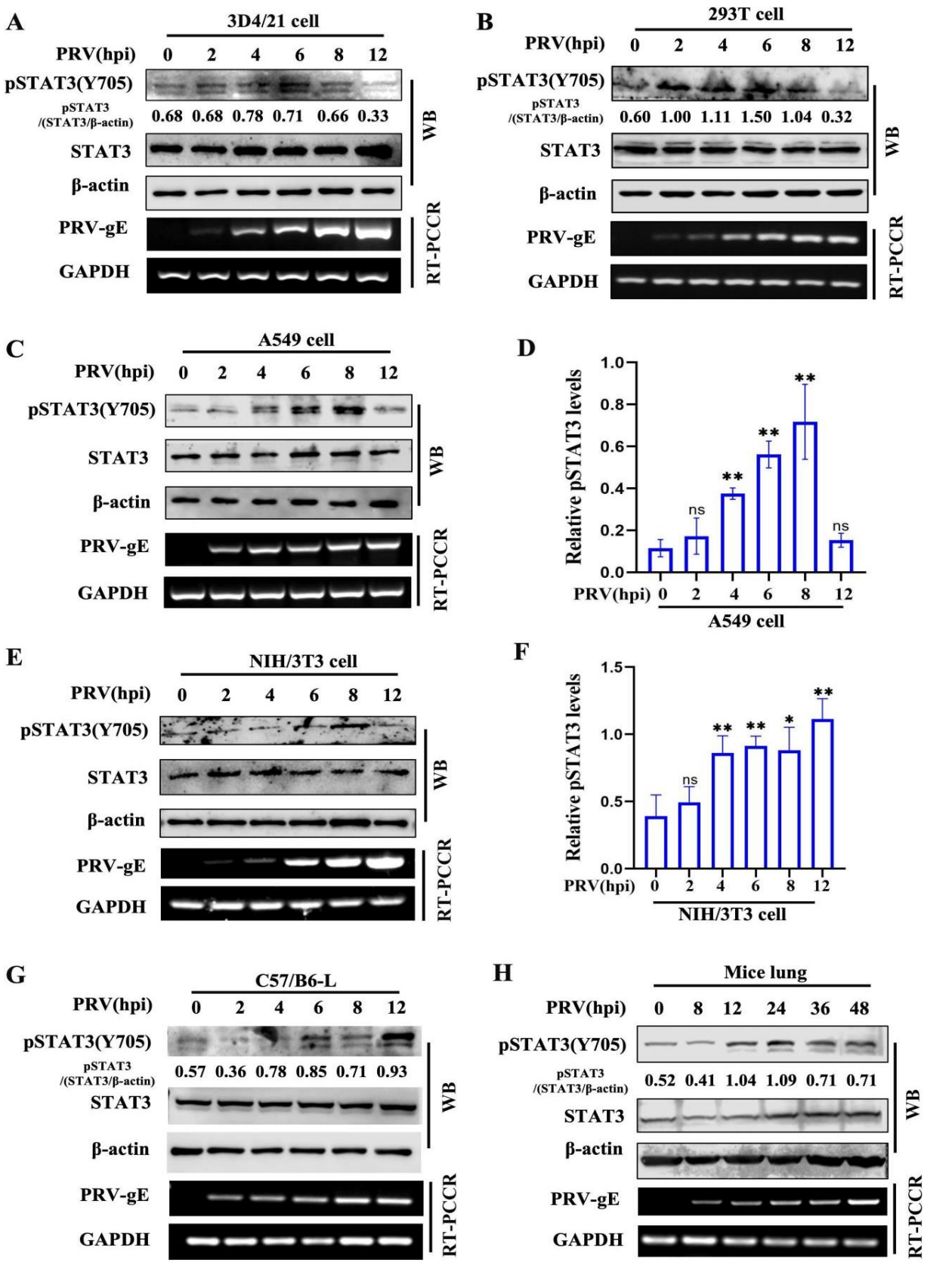



**Fig.1:** Phosphorylation of STAT3 at Y705 can be induced during PRV infection. (A) After infecting 3D4/21 cells with PRV (MOI=0.5) at indicated time points, the expression of PRV-gE was detected by RT-PCR. Phosphorylated STAT3 (pSTAT3-Y705) was detected via immunoblotting. Band intensities were quantified by densitometry and normalized to total STAT3 and β-actin levels. (B-D) 293T (B) or A549 (C, D) cells were infected with PRV (MOI=0.5) at indicated time points. pSTAT3 was detected by immunoblots (B and C) and quantitated by densitometry as described in Fig.1A (B and D). Data are represented as means±SD from three independent experiments (D). **p < 0.01. ns, no significant. (E-G) Immunoblots were utilized to detect pSTAT3 in PRV-infected NIH/3T3 (E and F) and C57/B6-L (G) at the indicated time points. Additionally, pSTAT3 levels were densitometry as described in Fig.1C (F, G). Data are represented as means±SD from three independent experiments (F). (H) Wild-type (WT) BALB/c mice (5-6 weeks, n = 5-7) were intranasally inoculated with PRV at a dose of $5\times10^4$ PFU for indicated time points. pSTAT3 in the lungs was detected via immunoblotting and quantified by densitometry as described in Fig.1A.

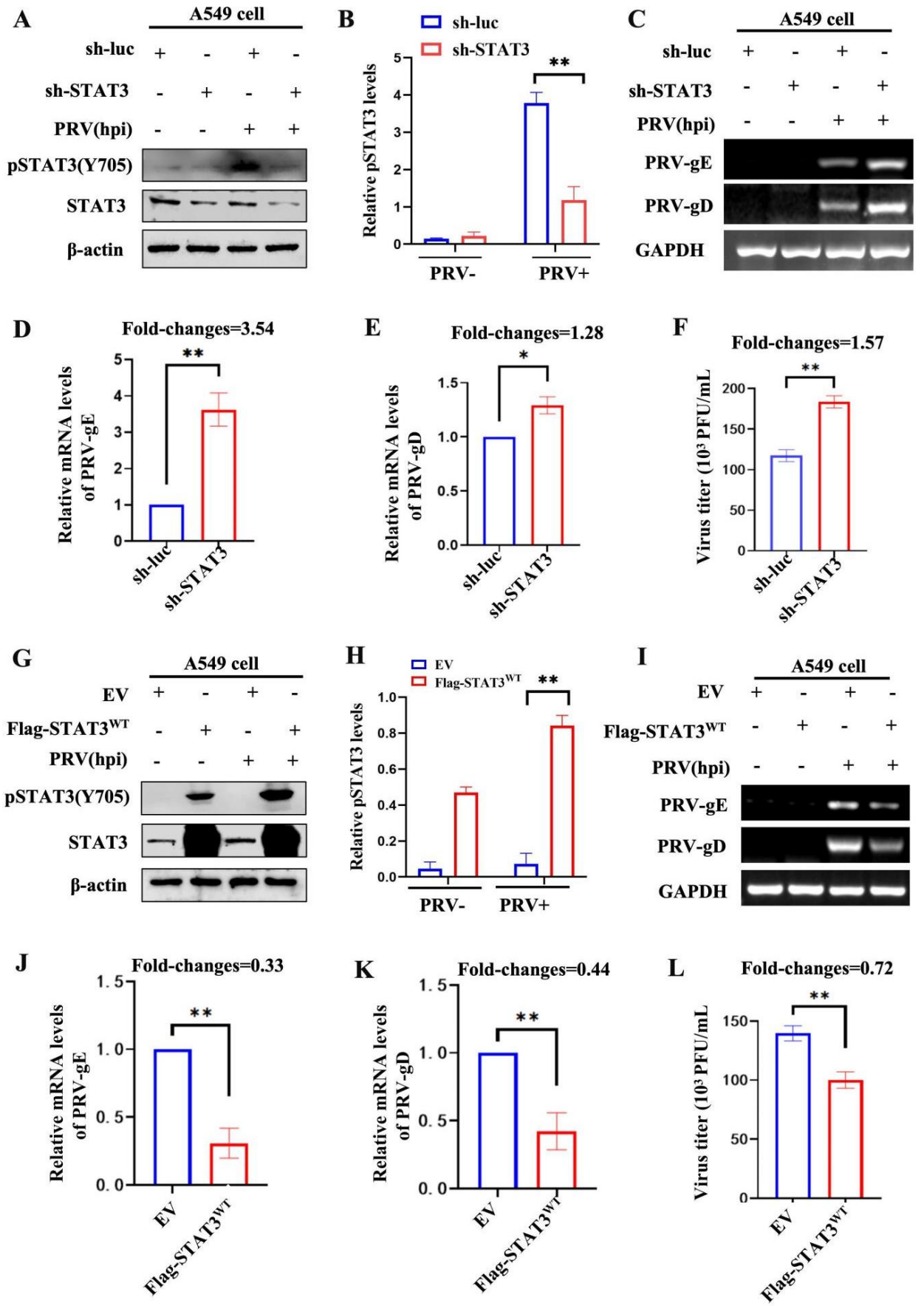



**Fig.2:** STAT3 could effectively inhibit the replication of PRV. (A-F) A549 cells stably expressing STAT3-specific shRNA were infected with or without PRV at an MOI of 0.5 for 12h. pSTAT3 was determined by immunoblotting and quantified via densitometry as described in Fig.1D (B). RT-PCR (C) and qRT-PCR (D and E) were performed to measure the mRNA abundance of PRV-gE and PRV-gD. Viral titers in cell supernatants (SNs) were measured using a plaque assay (F). (G-L) A549 cells transfected with Flag-tagged $STAT3^{WT}$, $STAT3^{Y705F}$, and EV were infected with PRV at the MOI of 0.5 for 12h. pSTAT3 was determined by immunoblotting (G) and quantified via densitometry as described in Fig.1D (H). The mRNA levels of PRV-gE and PRV-gD were analyzed by RT-PCR (I) and qRT-PCR (J and K), respectively. Viral titers from the cell SNs were determined by plaque assay (L).

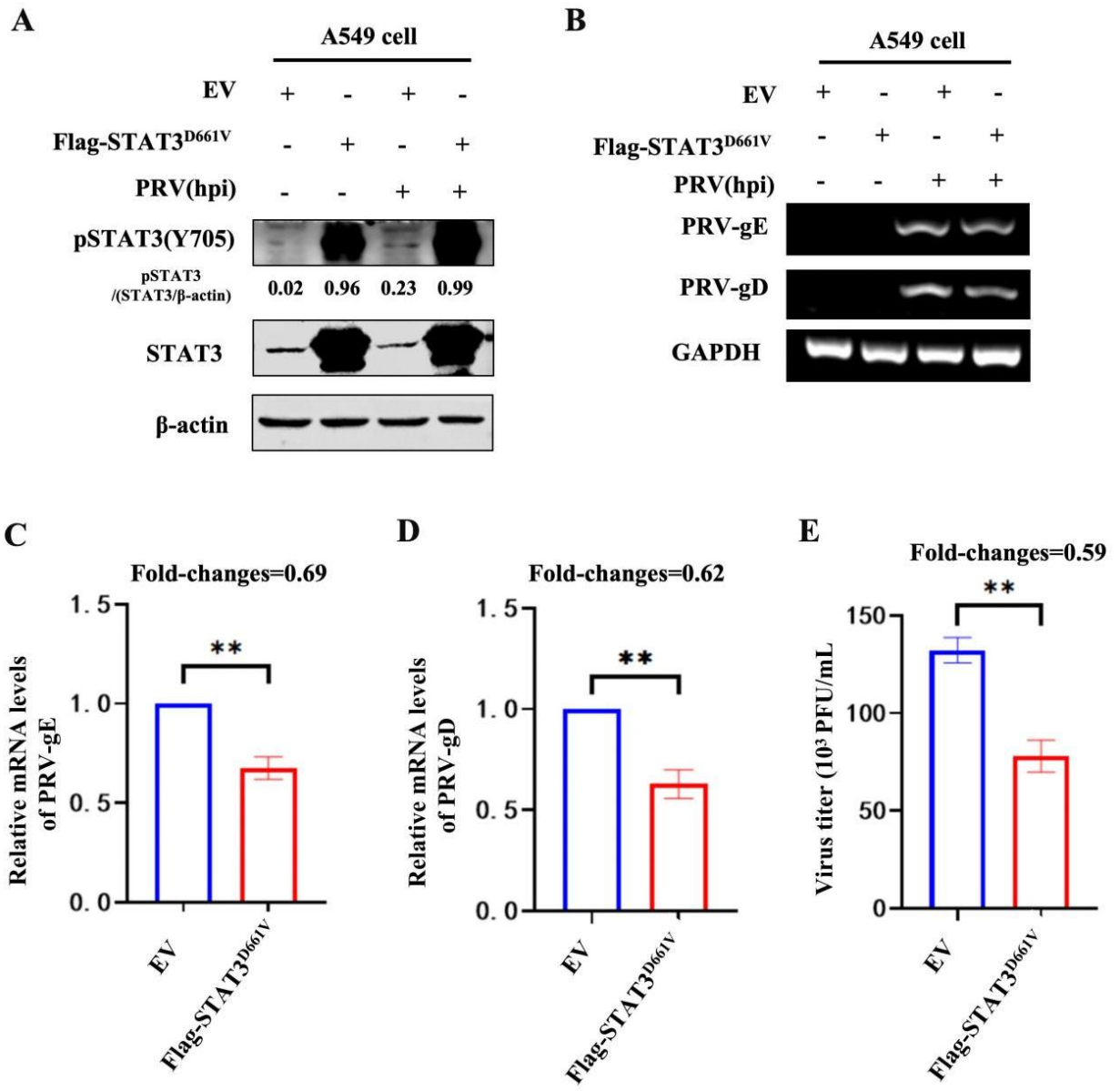



**Fig.3:** Constitutively active STAT3 markedly suppresses PRV replication. (A-E) A549 cells were transfected with plasmids overexpressing STAT3$^{D661V}$ (Flag-STAT3$^{D661V}$), or empty vector (EV), followed by PRV (MOI=0.5) infected for 12h. pSTAT3 levels were analyzed by immunoblots and quantitated by densitometry as described in Fig.1D (A). The mRNA expression of PRV-gE and PRV-gD were performed to assess the mRNA expression of RT-PCR (B) or qRT-PCR (C and D). Viral titers from the cell SNs were determined by plaque assay (E).

Collectively, these results demonstrate that constitutively active STAT3 efficiently suppresses the production of infectious PRV progeny virions in A549 cells, suggesting that STAT3 functions as a negative regulator of PRV replication.

**Disruption of STAT3 Y705 effectively facilitates the replication of PRV:** To investigate the regulatory function of STAT3 Y705 site during PRV infection, we generated a stable A549 cell line overexpressing Y705-mutated STAT3 (STAT3$^{Y705F}$). Both the IL-6-stimulation and PRV-infection assays confirmed the successful construction of this point-mutant cell line (Fig. 4A-4C). The established STAT3$^{Y705F}$-overexpressing cell line was subsequently subjected to PRV infection. Our data showed that disruption of STAT3 Y705 significantly elevated the mRNA levels of PRV gE and gD relative to EV control cells (Fig. 4D). Further qRT-PCR indicated that impaired STAT3 Y705 phosphorylation markedly enhanced the transcription of these two viral genes (PRV-gE, Fold-changes=1.57; PRV-gD, Fold-changes=8.23; Fig. 4E and 4F). Furthermore, viral titers in cell culture SNs harvested from STAT3$^{Y705F}$-overexpressing A549 cells was significantly higher than those from control cells, further confirming the pro-replicative effect of the STAT3-Y705F mutant on PRV replication (Fold-changes=1.43, Fig. 4G).

In summary, these findings demonstrate that disruption of STAT3 Y705 phosphorylation effectively facilitates PRV replication.

**STAT3$^{Y705F/+}$ mice exhibit increased susceptibility to PRV challenge:** To further elucidate the physiological function of STAT3 in response, we STAT3$^{Y705F/+}$ mice were utilized as previously described (Liu *et al.*, 2023). Both total STAT3 protein and pSTAT3 levels were markedly reduced in the lung and brain tissues of STAT3$^{Y705F/+}$ mice compared with WT littermates (Fig. 5A and 5B). Survival analysis revealed that STAT3$^{Y705F/+}$

mice were more susceptible to PRV infection. All mutant mice succumbed to death within 72hpi, whereas 40% of WT mice remained alive at this time point, with full mortality in WT mice not occurring until 96hpi (Fig. 5C). Consistent with the *in vitro* findings, the mRNA levels of PRV-gE significantly increased in the lungs (Fold-changes=2.02, Fig. 5D and 5E) and brains (Fold-changes=2.12, Fig. 5D and 5F) from STAT3$^{Y705F/+}$ mice relative to WT controls, indicating enhanced PRV replication in mutant mice. Taken together, these *in vivo* findings demonstrate that STAT3$^{Y705F/+}$ mice exhibit increased susceptibility to PRV challenge.

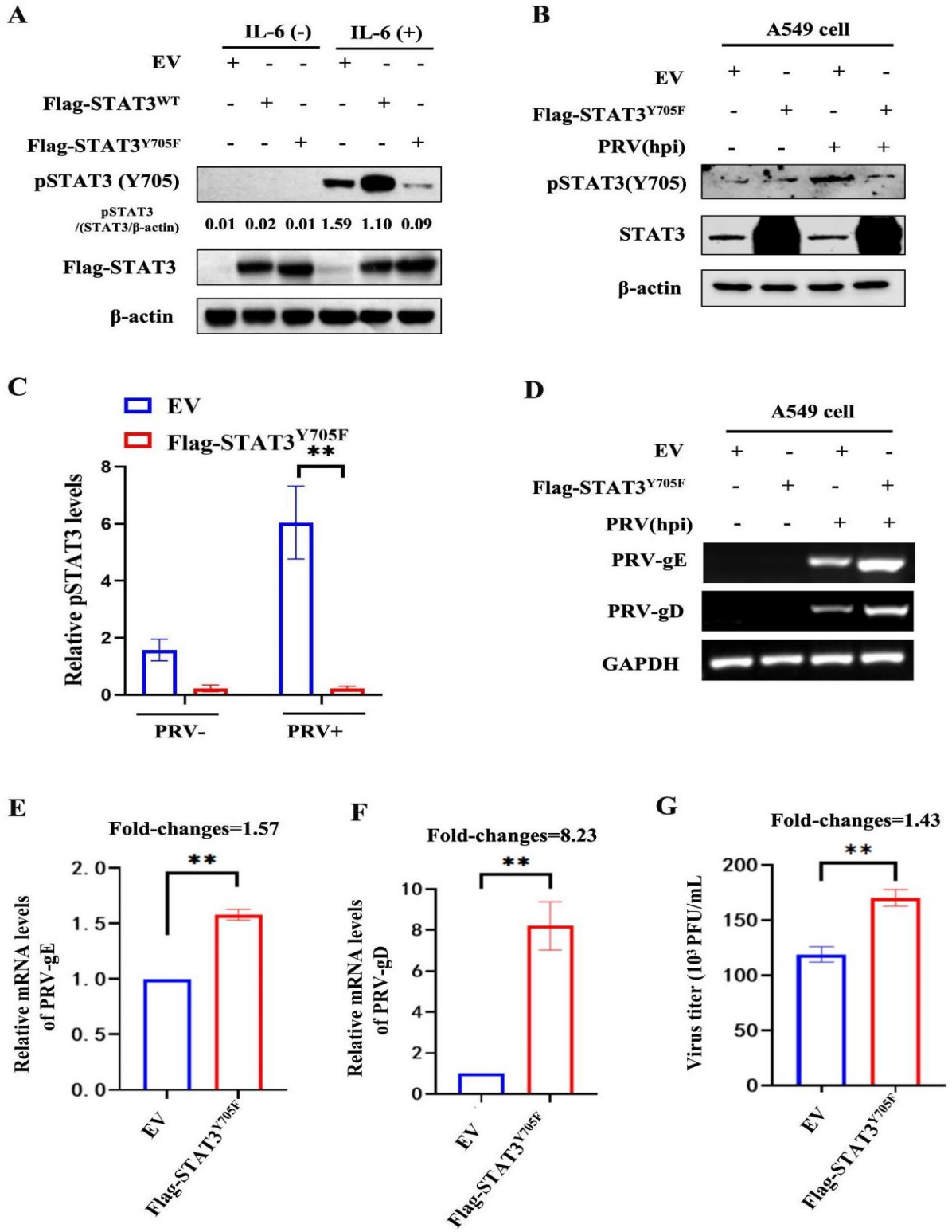



**Fig.4:** Disruption of STAT3 Y705 effectively facilitates the replication of PRV. (A) A549 cells were transfected with plasmids encoding STAT3$^{WT}$ (Flag-STAT3$^{WT}$), STAT3$^{Y705F}$ (Flag-STAT3$^{Y705F}$), or EV, followed by IL-6 stimulation for 2h. pSTAT3 levels were analyzed by immunoblots and quantitated by densitometry as described in Fig.1C. (B-G) A549 cells transfected with Flag-tagged STAT3$^{WT}$, STAT3$^{Y705F}$, and EV were infected with PRV at the MOI of 0.5 for 12h. pSTAT3 levels were analyzed by immunoblots (B) and quantitated by densitometry as described in Fig.1D (C). To quantify the mRNA expression of PRV-gE and PRV-gD, RT-PCR (D) and qRT-PCR (E and F) were performed. To examine the viral titers in cell SNs, plaque assay was used (G).

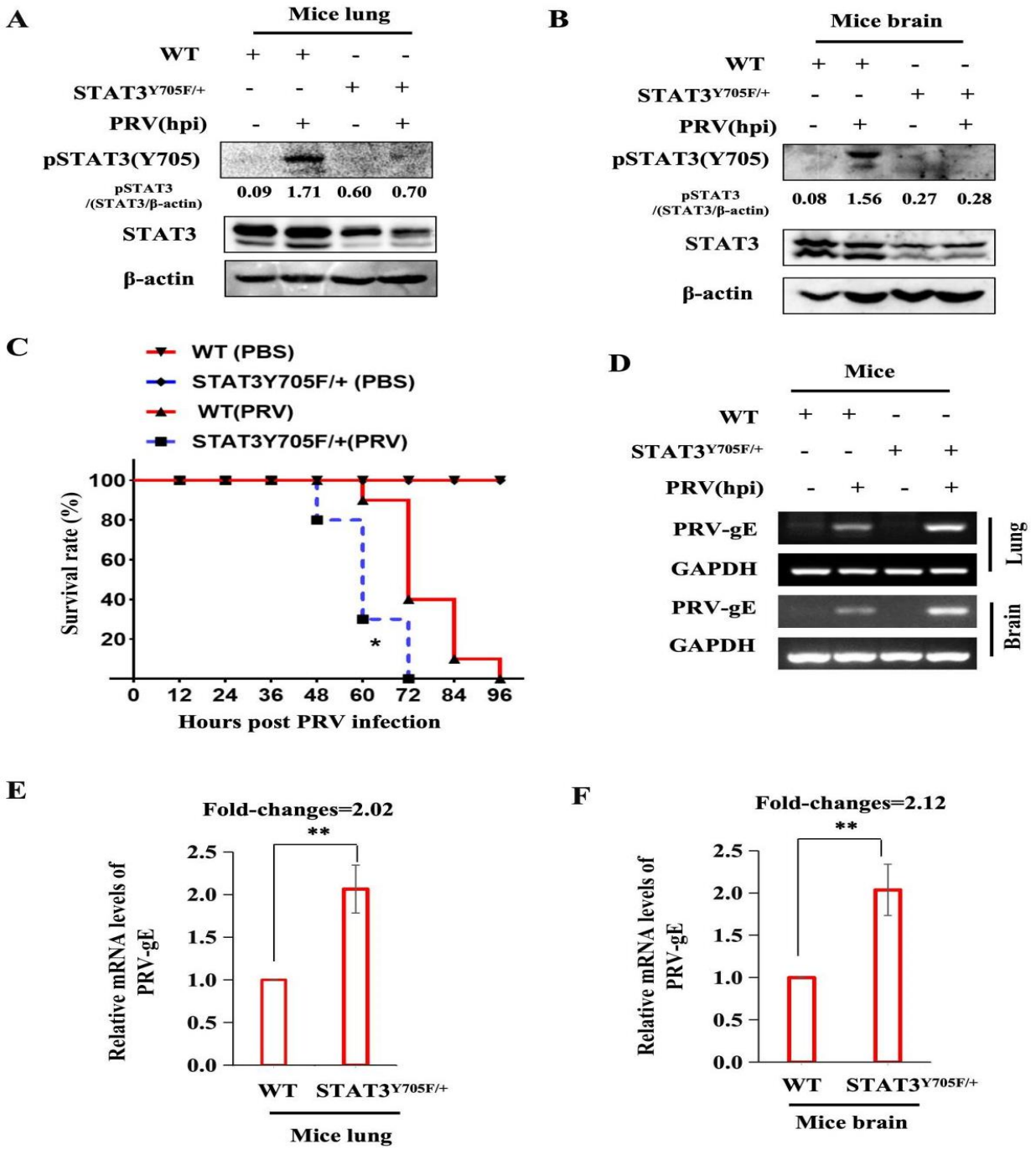



**Fig.5:** STAT3$^{Y705F/+}$ mice exhibit increased susceptibility to PRV challenge. (A and B) WT and STAT3$^{Y705F/+}$ mice (n= 5-6 per genotype for each group) were intranasally inoculated with PRV at a dose of $5\times10^4$ PFU for 48h. pSTAT3 levels in lungs (A) and brains (B) from PRV-infected WT and STAT3$^{Y705F/+}$ mice were analyzed by immunoblots (A and B) and quantitated by densitometry as described in Fig.1D (A and B). (C) The survival rates of WT and STAT3$^{Y705F/+}$ mice (n= 7 per genotype for each group) were monitored after intranasal inoculation with PRV. The log-rank (Mantel-Cox) test was applied to analyze group differences. (D-F) RT-PCR (D) or qRT-PCR (E and F) was utilized to analyze the mRNA levels of the viral genes PRV-gE and PRV-gD in lung (D, E) and brain (D, F) tissues from PRV-infected WT and STAT3$^{Y705F/+}$ mice (n= 5 per genotype for each group).

**Phosphorylation of STAT3 enhances the expression of some critical ISGs in response to PRV infection:** To further elucidate the function of STAT3 activation in host antiviral responses, we investigated the regulatory effect of STAT3 on the expression of critical ISGs (IFITM1, IFIT2, and ISG15). Our results showed that upon PRV infection, the mRNA expression levels of these ISGs were markedly downregulated in STAT3-knockdown 293T cells relative to control cells (Fig. 6A), and the consistent tendency was further validated in A549 cells (Fig. 6B). Conversely, STAT3 overexpression significantly increased the mRNA levels of IFITM1, IFIT2, and ISG15 in PRV-infected A549 cells (Fig. 6C). To further corroborate these results, we tested the expression of these ISGs in STAT3$^{D661V}$-overexpression 293T cells following PRV challenge. Notably, constitutively active STAT3 strongly enhanced the mRNA abundance of the three ISGs after PRV infection (Fig. 6D) , and identical results were observed in A549 cells (Fig. 6E). Furthermore, disruption of STAT3 Y705 observably attenuated the transcriptional levels of IFITM1, IFIT2, and ISG15 in PRV-infected A549 cells (Fig. 6F). Together, these data elucidate that STAT3 Y705 phosphorylation facilitates the expression of critical ISGs to initiate antiviral responses against PRV infection.

**STAT3 increases the expression of IL-6 in the cells infected with PRV**: Excessive inflammatory responses triggered by viral infection, including the overproduction of IL-6, are critically involved in viral pathogenesis (Rose-John *et al.*, 2023). Given our previous finding that STAT3 suppresses PRV replication, we further investigated whether STAT3 modulates the expression of key inflammatory cytokines, with a particular focus on IL-6. In STAT3-knockdown A549 cells, both RT-PCR (Fig. 7A) and qRT-PCR (Fig. 7B) results demonstrated that STAT3 depletion markedly reduced IL-6 mRNA levels in PRV-infected A549 cells (Fold-changes=0.32, Fig. 7B) relative to control cells. Conversely, STAT3 overexpression significantly upregulated IL-6 expression in PRV-challenged A549 cells (Fold-changes=4.17, Fig. 7C and 7D). Consistently, constitutively active STAT3 strongly elevated IL-6 mRNA abundance upon PRV infection (Fold-changes=2.92, Fig. 7E and 7F). Notably, mutation of the STAT3 Y705 site prominently diminished IL-6 mRNA expression in PRV-infected A549 cells (Fold-changes=0.05, Fig. 7G and 7H). Taken together, these observations indicate that STAT3 robustly increases IL-6 expression in the cells infected with PRV.

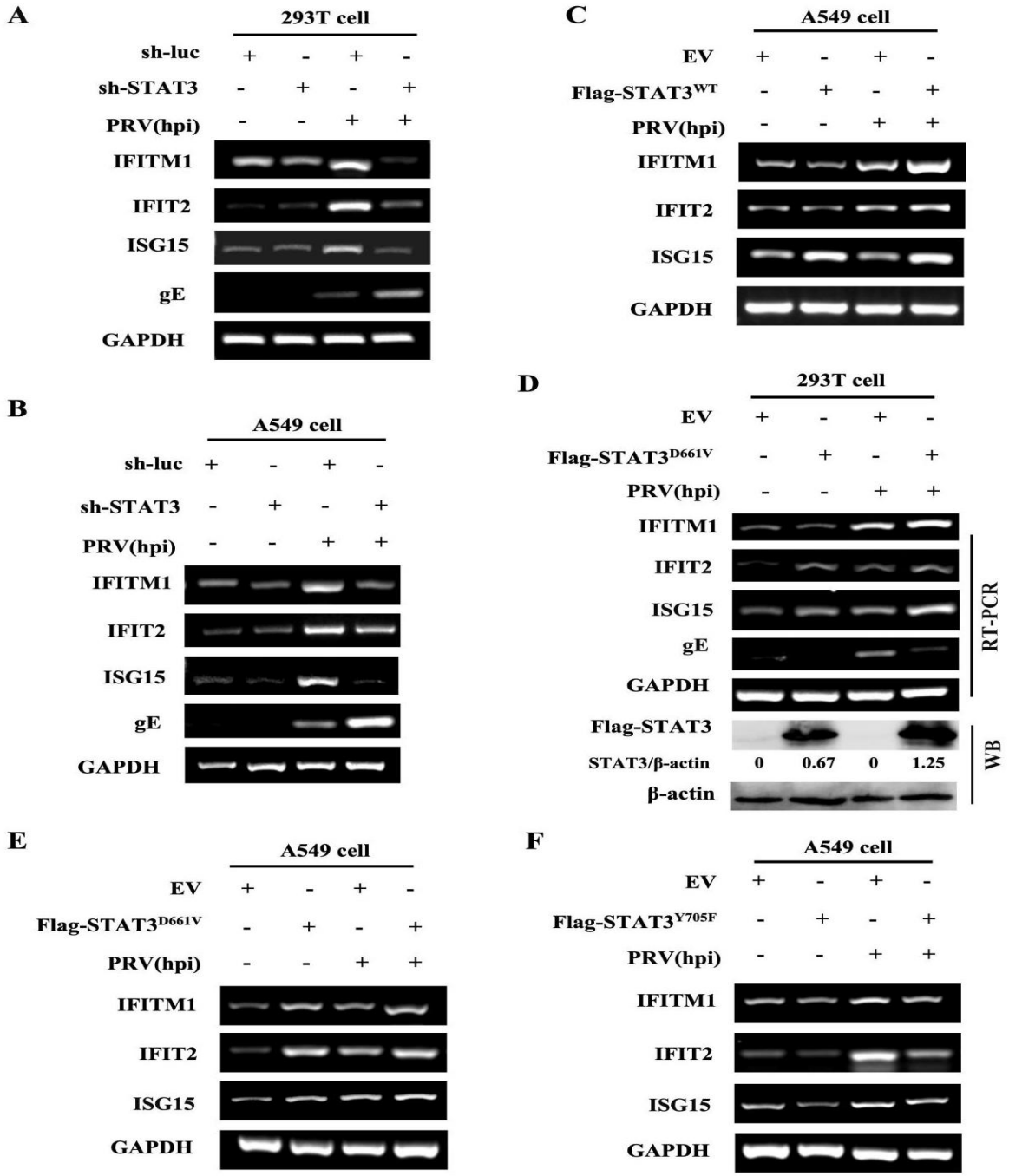



**Fig.6:** Phosphorylation of STAT3 enhances the expression of some critical ISGs in response to PRV infection. (A and B) RT-PCR was carried out to assess transcript abundances of ISGs (IFITM1, IFIT2, and ISG15) in STAT3-knockdown 293T cells (A) or A549 cells (B) with PRV infection at an MOI of 0.5. (C) RT-PCR measurements were conducted to quantify ISG transcript levels in PRV-challenged A549 cells with STAT3 overexpression. (D and E) Expression of IFITM1, IFIT2 and ISG15 transcripts was examined via RT-PCR in PRV-infected 293T cells (D) or A549 cells (E) overexpressing Falg-STAT3$^{D661V}$. STAT3 levels were analyzed by immunoblots and quantitated by densitometry as described in Fig.1A (E). (F) The mRNA levels of IFITM1, IFIT2, and ISG15 in STAT3$^{Y705F}$-overexpressing A549 cells with PRV infection were analyzed by RT-PCR.

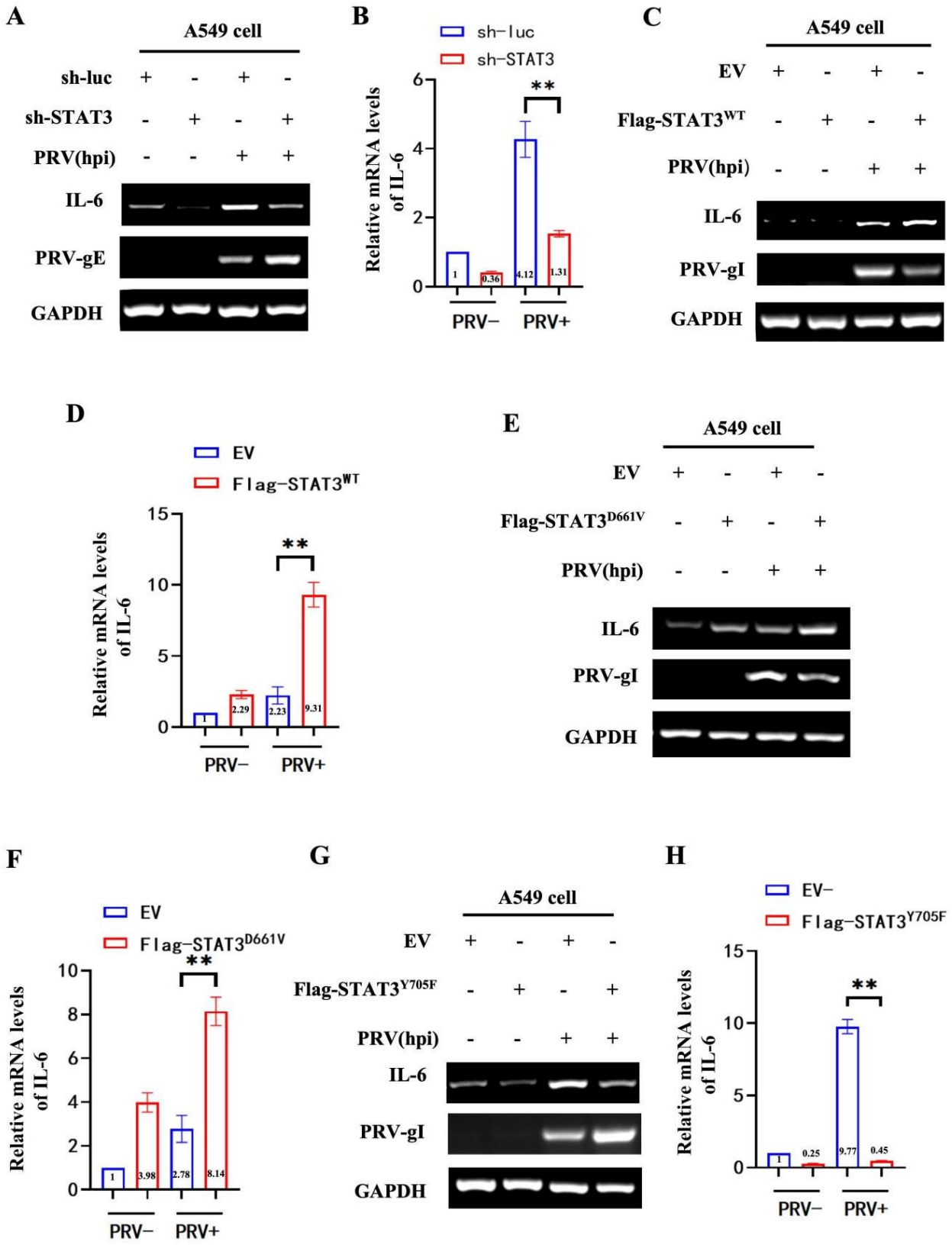



**Fig.7:** STAT3 increases the expression of IL-6 in the cells infected with PRV. (A and B) RT-PCR (A) or qRT-PCR (B) was carried out to assess transcript abundances of IL-6 in STAT3-knockdown A549 cells with PRV infection (MOI=0.5). (C and D) The mRNA levels of IL-6 were determined by RT-PCR (C) or qRT-PCR (D) in PRV-challenged A549 cells overexpressing $STAT3^{WT}$. (E and F) RT-PCR (E) or qRT-PCR (F) was employed to detect the mRNA levels of IL-6 in PRV-infected A549 cells with ectopic $STAT3^{D661V}$ expression. (G and H) RT-PCR (G) and qRT-PCR (H) utilized to assess IL-6 transcript levels in $STAT3^{Y705F}$-overexpressing A549 cells with PRV infection.

## DISCUSSION

PRV causes severe disease and imposes substantial economic losses on the global swine industry (Freuling *et al.*, 2017). To establish persistent infection, PRV has evolved diverse mechanisms to circumvent host innate immune responses. For example, the viral UL13 kinase facilitates STING ubiquitination and subsequent IRF3

phosphorylation, ultimately suppressing IFN signaling (Bo *et al.*, 2020). In addition, the viral gE protein triggers CBP degradation, which impedes IFN production (Lu *et al.*, 2021). STAT3 is a pivotal transcription factor regulating cell growth and differentiation, and its role during viral infection has drawn wide attention. α-herpesviruses like VZV activate STAT3 phosphorylation to upregulate survivin and facilitate viral replication (Buckingham *et al.*, 2018). γ-herpesviruses have more complex interactions with STAT3: viral IFN regulatory factor 1 (vIRF-1) blocks STAT3 phosphorylation via binding TYK2 (Yang *et al.*, 2023), while EBV activates STAT3 via LMP1 to drive viral gene expression (Liao e*t al.*, 2024; Xu *et al.,* 2025). To date, the interaction between STAT3 and PRV remains unreported.

This study demonstrated that PRV infection regulates STAT3 phosphorylation. Our data revealed that PRV infection significantly triggered STAT3 phosphorylation in a time-dependent manner in both A549 and 293T cells. Concordantly, similar increases in phosphorylated STAT3 were observed in murine NIH/3T3 cells and L929 cells. Consistent with these *in vitro* findings, PRV infection also induced STAT3 phosphorylation in BALB/c mice *in vivo*. We next investigated the functional role of STAT3 during PRV replication. Knockdown of STAT3 enhanced PRV replication, whereas STAT3 overexpression markedly suppressed viral proliferation. Moreover, constitutively active STAT3 significantly impeded PRV propagation, while overexpression of a dominant-negative STAT3 mutant accelerated PRV replication. To validate these findings *in vivo*, $STAT3^{Y705F/+}$ mice were employed. Compared with WT mice, $STAT3^{Y705F/+}$ mice displayed increased susceptibility to PRV infection, suggesting that impaired Y705 phosphorylation of STAT3 promotes PRV replication and aggravates viral pathogenesis *in vivo*. Collectively, these results firmly established that activated-STAT3 functions as an antiviral factor to constrain PRV replication.

We further investigated the role of PRV-triggered STAT3 phosphorylation in antiviral innate immunity. We assessed the transcriptional levels of several pivotal antiviral genes, including IFITM1, IFIT2, and ISG15. Our findings revealed that STAT3 silencing remarkably suppressed the expression of these antiviral genes, whereas STAT3 overexpression potentiated their transcription. Similarly, constitutively active STAT3 strongly facilitated the induction of these antiviral genes. In contrast, the STAT3-Y705F point mutation greatly blunted their upregulation following PRV infection. These data suggest that STAT3 positively regulates ISGs transcription, though the precise underlying mechanism remains to be further elucidated. Future studies including promoter-binding/ chromatin immunoprecipitation (ChIP) or reporter assays will be implemented to clarify whether STAT3 directly modulates these ISGs. IL-6 is a multifunctional cytokine that serves a pivotal role in host defense, inflammatory responses, and immune regulation (Jones *et al.*, 2018). To clarify whether STAT3 regulates IL-6 expression, we conducted functional assays using cell lines with STAT3 knockdown, overexpression, constitutive activation, or Y705F mutation. We observed that STAT3 phosphorylation triggered upon PRV infection significantly promoted IL-6 expression.

In conclusion, this study systematically delineates the dynamic changes and antiviral function of the STAT3 signaling pathway during PRV infection. We validate that PRV infection induces elevates STAT3 phosphorylation, and that activated-STAT3 restricts PRV replication by positively regulating ISGs such as IFITM1, IFIT2, and ISG15. These findings not only advance our knowledge of virus-host regulatory networks, but also offer mechanistic insights into PRV pathogenesis.

**Authors Contribution:** S.L. conceived the study, acquired funding and secured resources. F.Q., H.Z., F.X., B.W. & Z.A. handled software, analysis, methodology and validation. S.L., F.Q. drafted; R.S., H.D. supervised, revised and managed the project. All authors approved the final manuscript.

**Funding:** The present study received support from the National Natural Science Foundation of China (32473048), and the Science and Technology Innovation Project of Fujian Agriculture and Forestry University (KFB25006A).

**Institutional Review Board Statement:** Approval for the animal care and experimental protocol was granted by the Regulation of College of Animal Sciences, Fujian Agriculture and Forestry University of Research Ethics Committee (Permit No. PZCASFAFU24017).

**Informed Consent Statement:** Not applicable.

**Data Availability Statement:** This study did not generate or analyze new data, and data sharing is not applicable to this manuscript.

**Generative AI statement:** No generative AI was used by the authors during the preparation of this manuscript.

**Conflicts of Interest:** The authors report no conflicts of interest.

## REFERENCES

Bo Z, Miao Y, Xi R, *et al.*, 2020. PRV UL13 inhibits cGAS-STING-mediated IFN-β production by phosphorylating IRF3. Veterinary Research 51(1):118.

Buckingham EM, Girsch J, Jackson W, *et al.*, 2018. Autophagy quantification and STAT3 expression in a human skin organ culture model for innate immunity to herpes zoster. Frontiers in Microbiology 9:2935.

Chen H, Fan J, Sun X, *et al.*, 2023. Characterization of pseudorabies virus associated with severe respiratory and neuronal signs in old pigs. Transboundary and Emerging Diseases 2023:8855739.

Chen X, Kong N, Xu J, *et al.,* 2021. Pseudorabies virus UL24 antagonizes OASL-mediated antiviral effect. Virus Research 295: 198276.

Chi X, Huang G, Wang L, *et al.*, 2024. A small protein encoded by PCBP1-AS1 is identified as a key regulator of influenza virus replication via enhancing autophagy. PLoS Pathogens 20(8):e1012461.

Faust Akl C, Andersen BM, Li Z, *et al.*, 2025. Glioblastoma-instructed astrocytes suppress tumour-specific T cell immunity. Nature 643(8070):219-229.

Freuling CM, Müller TF, Mettenleiter TC, 2017. Vaccines against pseudorabies virus (PrV). Veterinary Microbiology 206:3-9.

Gu R, Xu E, Hong J, *et al.*, 2025. Expression of NEAT1 induced by influenza virus infection is regulated by activated STAT3 and contributes to STAT3-mediated antiviral immunity. Frontiers in Immunology 16:1693884.

Holicek P, Guilbaud E, Klapp V, *et al.*, 2024. Type I interferon and cancer.

Immunological Reviews 321(1):115-127.
Hu Y, Dong Z, Liu K, 2024. Unraveling the complexity of STAT3 in cancer: molecular understanding and drug discovery. Journal of Experimental & Clinical Cancer Research 43(1):23.
Jones SA, Jenkins BJ, 2018. Recent insights into targeting the IL-6 cytokine family in inflammatory diseases and cancer. Nature Reviews Immunology 18(12):773-789.
Laval K, Enquist LW, 2020. The neuropathic itch caused by pseudorabies virus. Pathogens 9 (4): 254.
Li A, Lu G, Qi J, *et al.*, 2017. Structural basis of nectin-1 recognition by pseudorabies virus glycoprotein D. PLoS Pathogens 13(5):e1006314.
Li C, He WF, Li LX, *et al.,* 2022. Interferon-stimulated gene 15 knockout in mice impairs IFNα-mediated antiviral activity. Viruses 14(9): 1862.
Liao Y, Yan J, Beri NR, *et al.*, 2024. Germinal center cytokine driven epigenetic control of Epstein-Barr virus latency gene expression. PLoS Pathogens 20(4):e1011939.
Liu A, Xue T, Zhao X, *et al.*, 2022a. Pseudorabies virus associations in wild animals: Review of potential reservoirs for cross-host transmission. Viruses 14(10): 2254.
Liu H, Li C, He W, *et al.*, 2022b. Free ISG15 inhibits pseudorabies virus infection by positively regulating type I IFN signaling. PLoS Pathogens 18(10):e1010921.
Liu Q, Kuang Y, Li Y, *et al.*, 2022c. The epidemiology and variation in pseudorabies virus: A continuing challenge to pigs and humans. Viruses 14(7):1463.
Liu SS, Liu SY, Yu Z, *et al.*, 2023. STAT3 regulates antiviral immunity by suppressing excessive interferon signaling. Cell Reports 42(7):112806.
Lu M, Qiu S, Zhang L, *et al.*, 2021. Pseudorabies virus glycoprotein gE suppresses interferon-β production via CREB-binding protein degradation. Virus Research 291:198220.
Ma Y, Guo G, Li T, *et al.*, 2022. A novel imatinib-upregulated long noncoding RNA plays a critical role in inhibition of tumor growth induced by Abl oncogenes. Molecular Cancer 21(1):5.
Ma Z, Bai J, Jiang C, *et al.*, 2023. Tegument protein UL21 of alpha-herpesvirus inhibits the innate immunity by triggering CGAS degradation through TOLLIP-mediated selective autophagy. Autophagy 19(5):1512-1532.
Mahony R, Gargan S, Roberts KL, *et al.*, 2017. A novel anti-viral role for STAT3 in IFN-α signalling responses. Cell and Molecular Life Sciences 74(9):1755-1764.
Mohiuddin MM, Singh AK, Scobie L, *et al.*, 2023. Graft dysfunction in compassionate use of genetically engineered pig-to-human cardiac xenotransplantation: a case report. Lancet 402(10399):397-410.
Musante AR, Pedersen K and Hall P, 2014. First reports of pseudorabies and winter ticks (Dermacentor albipictus) associated with an emerging feral swine (Sus scrofa) population in New Hampshire. Journal of Wildlife Diseases 50(1):121-124.
Neurath MF, 2024. Strategies for targeting cytokines in inflammatory bowel disease. Nature Reviews Immunology 24(8):559-576.
Oda K, Hatori Y, Kodama A, Uchiyama S, *et al.*, 2025. Molecular basis of IFN-γ-induced STAT3 phosphorylation stimulated by Sendai virus C protein. Journal of Biological Chemistry 301(11):110744.
Papageorgiou K, Stoikou A, Papadopoulos DK, *et al.*, 2024. pseudorabies virus prevalence in lung samples of hunted wild boars in Northwestern Greece. Pathogens 13(11): 929.
Roca Suarez AA, Van Renne N, Thomas F. Baumert *et al.*, 2018. Viral manipulation of STAT3: Evade, exploit, and injure. PLoS Pathogens 14(3):e1006839.
Rose-John S, Jenkins BJ, Garbers C, *et al.*, 2023. Targeting IL-6 trans-signalling: past, present and future prospects. Nature Reviews Immunology 23(10):666-681.
Wang C, Li L, Zhai X, *et al.*, 2024. Evasion of the antiviral innate immunity by PRV. Int J Mol Sci 25(23):13140.
Wang J, Wang CF, Ming SL, *et al.,* 2020. Porcine IFITM1 is a host restriction factor that inhibits pseudorabies virus infection. International Journal of Biological Macromolecules 151:1181-1193.
Wang S, Luo X, Yan R, *et al.*, 2016. 3-Anhydro-6-hydroxy-ophiobolin A displays high in vitro and in vivo efficacy against influenza A virus infection. Protein & Cell 7(11):839-843.
Wang WB, Levy DE and Lee CK, 2011. STAT3 negatively regulates type I IFN-mediated antiviral response. Journal of Immunology 187(5):2578-2585.
Wang Y, Chen G, Pan D, *et al.*, 2024. Pig-to-human kidney xenotransplants using genetically modified minipigs. Cell Rep Med 5(10):101744.
Xie J, Bi Y, Xu S, *et al.*, 2020. Host antiviral protein IFITM2 restricts pseudorabies virus replication. Virus Research 287:198105.
Xu H, Koganti S, Li C, McIntosh MT, *et al.*, 2025. STAT3, MYC, and EBNA1 cooperate through a ZC3H18 transcriptional network to regulate survival and proliferation of EBV-positive lymphomas. PLoS Pathogens 21(5):e1013166.
Yan W, Hu Z, Zhang Y, *et al.*, 2023. Metagenomic next-generation sequencing for diagnosis of human encephalitis and endophthalmitis caused by pseudorabies virus. Frontiers in Medicine 8:753988.
Yang Z, Xiang Q, Nicholas J, *et al.,* 2023. Direct and biologically significant interactions of human herpesvirus 8 interferon regulatory factor 1 with STAT3 and Janus kinase TYK2. PLoS Pathogens 19(11):e1011806.
Ye N, Feng W, Fu T, *et al.*, 2023. Membrane fusion, potential threats, and natural antiviral drugs of pseudorabies virus. Veterinary Research 54(1):39.
Yin Y, Romero N, Favoreel HW, 2021. Pseudorabies virus inhibits type i and type iii interferon-induced signaling via proteasomal degradation of janus kinases. Journal of Virology 95(20):e0079321.
Yoshida T, Latt KZ, Rosenberg AZ, *et al.*, 2024. PKR activation-induced mitochondrial dysfunction in HIV-transgenic mice with nephropathy. Elife 12:RP91260.
Zhang N, Yan J, Lu G, *et al.*, 2011. Binding of herpes simplex virus glycoprotein D to nectin-1 exploits host cell adhesion. Nature Communications 2:577.
Zhang R, Tang J, 2021. Evasion of I interferon-mediated innate immunity by pseudorabies virus. Frontiers in Microbiology 12:801257.
Zou S, Tong Q, Liu B, *et al.*, 2020. Targeting STAT3 in cancer immunotherapy. Molecular Cancer 19(1):145.